

## PREDICTION OF SOLAR AND GEOMAGNETIC ACTIVITY FOR ESA LOW-FLYING SPACECRAFT

R. Mugellesi<sup>1</sup> and D. J. Kerridge<sup>2</sup>

<sup>1</sup> Spacecraft Trajectory Branch, ESA/ESOC/OAD, Darmstadt, FRG

<sup>2</sup> Geomagnetism Group, British Geological Survey, Edinburgh, Scotland

### ABSTRACT

During the planning and operations of low-altitude earth-orbit satellite missions, an important activity is orbit prediction over periods ranging from days to more than one year. It is also necessary to assess the impact of solar activity on the on-board electronics over the long-term. In the orbital propagation model, the dominant, and most difficult component to predict, is the drag force, as it is sensitive to the continuous variations of solar and geomagnetic activity. In the air density models presently available in ESOC, solar activity is parameterized in terms of the solar radio flux F10.7, whereas geomagnetic activity is represented by the  $K_p$  (or the equivalent  $a_p$ ) index. The availability of long-, medium- and short-term prediction of the solar and geomagnetic activity is fundamental for satisfying the current ESOC operational needs.

A method for medium- and long-term forecasting of the activities has been developed by the Geomagnetism Group of BGS (Edinburgh, UK) under ESA contract and implemented in the ESOC computer system. The method is a variant of the McNish & Lincoln technique and predicts monthly mean values of the F10.7 radio flux and  $a_p$  index. The SOLMAG software is currently used for mission analysis and in planning work for the ERS and EURECA missions. The performance of the prediction software is discussed.

predicted values of the solar and geomagnetic activities, although the ballistic coefficient is also frequently in doubt.

Density changes determine spacecraft lifetime. Reliable lifetime predictions are of great importance for any mission planning work. Lifetime in terms of years of on-station operation and reboost requirements are major drivers of system costs. Spacecraft control system design is influenced by the aerodynamic torque which, for large structures, becomes one of the dominant disturbances.

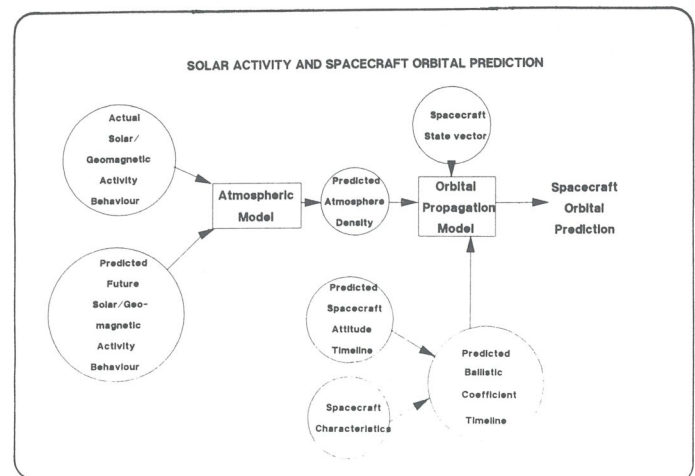


Figure 1. Solar activity and Spacecraft Orbital Prediction

### 1. MODELLING OBJECTIVES

Spacecraft orbital predictions are critically dependent on the ability to forecast future behaviour of solar and geomagnetic activity, as illustrated in Figure 1.

Current and predicted future values of these quantities are inputs to the atmospheric model used to compute the air density along the orbital path. Density values are combined with the predicted ballistic coefficient timeline to compute the drag force in the orbital propagation model and to predict orbital decay. The major uncertainty in making orbit predictions is due to errors in the

Air density predictions are also important for the quality of spacecraft experiments since gases, in particular atomic oxygen, can cause deterioration of exposed surfaces.

Communication with satellites is disrupted during times of ionospheric disturbances. The major disturbances are associated with increased emission of electromagnetic radiation from the sun. Such changes can be deleterious to both spacecraft to spacecraft and spacecraft to ground command and control communication, in particular tracking.

Measurements of the orbital parameters of early satellites established correlations between atmospheric density variations and both the F10.7 flux and the planetary magnetic activity index  $K_p$  (or the equivalent amplitude  $a_p$ ). This led to the development of atmospheric density models in which the effects of solar activity are parameterised by the F10.7 flux and the  $K_p$  index. The accuracy of orbital predictions made from such models depends on the ability to make successful forecasts of future values of the F10.7 flux and the  $K_p$  index.

Ideally, forecasts of the F10.7 flux and  $K_p$  index, or directly of upper atmospheric density, would be made on the basis of physical models of solar behaviour and solar-terrestrial interactions. However, the observational data sets that would be needed to achieve this, from monitoring of solar electromagnetic radiation and the transport of particles to the Earth by the solar wind, are not available, and, at present, the theory of the mechanisms that lead to atmospheric density changes is incomplete. In practice, forecasting of the F10.7 flux and the  $K_p$  index depends on identification of past patterns of behaviour of the indices themselves and correlations with other solar measurements. Extrapolations into the future are made on the basis of these patterns and relations.

The specific requirement for the study was to develop and implement a computer algorithm for forecasting solar and geomagnetic activity in the long and medium term. Predictions of the F10.7 solar radio flux and the  $a_p$  geomagnetic activity index were required since these are the input parameters to atmospheric density models used in ESOC.

## 2. THE DATA SET

### 2.1 Solar Activity Indices

The commonly used measures of solar activity are the sunspot number and the sun's radio emission in solar flux units. Sunspots are the most obvious features of the entire visible disk of the sun. Their existence had been suspected for some seventeen centuries before it was definitely confirmed by telescopic observations made in 1610 by Galileo and others. The spots commonly appear in groups and frequently in related pairs, where each group may contain as many as a hundred individual spots of different size and may extend for  $3 \times 10^5$  km. Each spot consists of a dark central area (umbra), which gives an indication of a lower temperature, surrounded by a less dark region (penumbra). The spots vary in size with the time: generally they start as small spots and increase to a maximum in a week or two; they appear to remain steady for a while and then shrink gradually over a period up to several months.

Variation with time in the number of spots, although noted by the ancient observers, was recognized as cyclic by the observations made by the German astronomer H. Schwabe in 1843. The cyclic nature was generally accepted around 1850, following the introduction by R. Wolf of the "relative sunspot number  $R_s$ " as a measure of solar activity:

$$R_s = k(10g + f) \quad (1)$$

where  $k$  is a normalization parameter which varies from one observatory to another, accounting for telescope size, atmospheric opacity, etc., in order to assure uniformity in the measures obtained by different stations;  $g$  is the number of the observed sunspot groups on the disk of the sun;  $f$  is the total number of sunspots observed regardless of size.

Wolf, director of the Swiss Federal Observatory in Zurich, established there the long tradition of the solar observations and applied his formula to the records of the historical observations as far back as 1749. For this reason  $R_s$  is also called the Zurich Sunspot Number, and it is indicated by  $R_Z$ . Beginning in December 1980, the International Sunspot Number, denoted  $R_I$ , came into use replacing  $R_Z$ .  $R_I$  is computed, using Equation (1), by the Sunspot Index Data Center in Brussels, Belgium, using data obtained from more than 25 observatories. These stations constitute an international network, with the Locarno station (Switzerland) used to provide continuity with the past Zurich series of  $R_Z$ .

Another measure of the sunspot activity is the American Relative Sunspot Number, whose monthly value is denoted by  $R_A$ . This is computed on the basis of observations made by the Solar Division of the American Association of Variable Star Observers, which is a rather small group of observers, mostly amateurs.

Because the sunspot number has been used for such a long time, with almost complete data going back to 1749, and partial data to 1610, it is still employed as a convenient index for recording variations in solar activity.

The daily numbers, based on Wolf's equation, are averaged to produce monthly mean sunspot numbers. While the former are the primary data, more often the latter are used for comparative studies. However, these monthly mean numbers still show considerable variation, so a smoothing technique has come into use which reduces the month to month scatter and shows the general trend of the solar activity with time. The Smoothed Sunspot Number, denoted  $\bar{R}$ , is a mean over 13 months and is defined as:

$$\bar{R} = (R_6 + R_{-6} + 2 \sum R_i) / 24 \quad (2)$$

where  $R_{+6}$  is the monthly mean sunspot number six months ahead of the month of interest,  $R_{-6}$  is the monthly mean sunspot number six months behind the month of interest, and the summation is taken over the monthly mean sunspot numbers five months either side and including the month of interest.  $\bar{R}$  can be based on either  $R_Z$ ,  $R_I$  or  $R_A$  values, although usually it is on the former.

Sunspot cycles, which by international convention, begin and end at sunspot minima, have an average length of about 11 years. The average ascent time, from minimum to maximum is approximately 50 months, the average



descent time, from maximum to minimum is about 80 months.

The other frequently used index of solar activity is the **Solar Flux F10.7**, that is the 10.7 cm wavelength solar radio emission. This index is obtained from daily observations, made at the Algoquin Radio Observatory near Ottawa, Canada, of the 2800 MHz radio emissions that originate from the solar disk and from any active region of the sun, expressed in solar flux units corrected to 1 AU ( $1.5 \times 10^8 \text{ km}$ ). The daily value is a single observation made near local noon at 17.00 UT. By replacing the sunspot numbers with the solar flux F10.7 values, equation (2) can be used to obtain the smoothed solar flux, denoted  $F_{10.7}$ .

## 2.2 Geomagnetic Activity Indices

The interaction of the solar wind and the earth's magnetic field is responsible for the perturbations of the geomagnetic field, called geomagnetic storms. Through this interaction, changes in the electric fields and currents in the ionosphere and magnetosphere are induced. These currents in turn produce magnetic disturbances, i.e. deviations from the quiet geomagnetic field, which are detected and recorded by magnetometers installed at observatories. Magnetic substorms are a subclass of geomagnetic storms, with effects most pronounced at auroral stations, caused by the auroral electrojet, the intense ionospheric currents flowing into the auroral zone. Dissipation of the electric currents and precipitation of energetic particles causes intense heating of the atmosphere. This is the dominant contributor to perturbations in the structure of the thermosphere.

Geomagnetic storms are somewhat correlated with sunspot activity: thus, a storm may recur after 27 days (the length of a solar rotation) and the overall activity tends to follow the 11-year solar cycle. In addition to large storms which can last several days, there are small and regular daily variations of the geomagnetic field correlated with the sun and the moon. Atmospheric solar and lunar tides produce motions in the ionosphere, and the resulting dynamo currents are accompanied by magnetic fields. These small magnetic fields are superimposed on the main geomagnetic field and represent the fairly regular daily fluctuations in the measured field strength at the Earth's surface.

The most commonly used global geomagnetic activity indices can be grouped into three categories according to the region from which the records used in their derivation come. These are as follows:

- Auroral zone: AE index,
- Middle-latitude zone: K/A-type indices and aa
- Low-latitude zone: Dst index.

In the mid-latitude observatories, 3-hourly ranges of the amplitude (expressed in units of nanoTeslas, where  $1 \text{ nT} = 10^{-5} \text{ Gauss}$ ) of the variation of the horizontal components of the geomagnetic field with respect to the quiet-day curve are measured. In order to obtain compa-

table results from different observatories, a standardization has been adopted, which consists of converting the observed amplitude of the variation to a **3-hourly index K**, an integer in the range 0 to 9. Each observatory references the records to a level which has been determined for it and expresses the most disturbed value of the 3-hourly range by the index K.

In Table 1 the range of the amplitude of the variation of the horizontal components at Fredericksburg observatory (USA) and the scale for the K index are shown. For example, if the most disturbed value for a given 3-hour interval is smaller than 5 nT then  $K=0$ ; if it is greater than 5 nT and less than 10 nT then  $K=1$ ; etc., and finally if it is greater than 500 nT then  $K=9$ .

amplitude (nT)	K
0 - 5	0
5 - 10	1
10 - 20	2
20 - 40	3
40 - 70	4
70 - 120	5
120 - 200	6
200 - 300	7
300 - 500	8
> 500	9

**Table 1. Amplitude Range and K Index for Fredericksburg**

The index K is not exactly the logarithm of the amplitude of the variation of the horizontal components, but expresses the geomagnetic disturbance on a quasi-logarithmic scale for each 3-hour UT interval. The K index has been introduced to give a measure of the particle emission from the sun, which has an effect quite different from that of the solar wave radiation. Therefore, in scaling K, only disturbance parameters are measured; that means the regular and predictable variations caused by the daily solar wave radiation, solar flare effects and other effects must be eliminated in scaling K.

From the 3-hour K indices, the corresponding **3-hour amplitude index  $a_k$**  can be derived. These indices express (in nanoTeslas) the amplitude of the variation of the horizontal components during a 3-hour interval.  $A_k$  is the daily average of the 8 values of  $a_k$ . Table 2 shows the conversion between  $a_k$  and K. The factor obtained by dividing the amplitude variation corresponding to  $K=9$  at a given station by the constant 250 is used to express  $a_k$  in nanoTeslas. For example, at Fredericksburg the amplitude variation for  $K=9$  is 500, and dividing by 250, the factor of 2 is obtained. Therefore, at this observatory,  $a_k$  is expressed in units of 2 nT ( $K=3$ ,  $a_k = 30$ ). The scale of Table 2 is used to convert the K indices for a standard station into  $a_k$  values where only the unit depends upon the station (the unit is 2 nT for a standard station).

K	$a_k$ (nT)
0	0
1	3
2	7
3	15
4	27
5	48
6	80
7	140
8	240
9	400

Table 2 Conversion between K and  $a_k$

The Planetary 3-hourly index  $K_p$  has been introduced by international agreement to characterize global geomagnetic activity. It is obtained by using the K indices obtained from 12 observatories situated at geomagnetic latitudes between 48 and 63 deg. The values of K reported from the observatories are then corrected for the station's geomagnetic latitude (since the activity is latitude dependent) and then averaged to produce the 3-hourly planetary index  $K_p$ . In order to express a wide range of geomagnetic activity by a one-digit number,  $K_p$  is expressed in 1/3 unit, i.e. it is subdivided into 28 grades:  $K_p = 0_0, 0+, 1-, 1_0, 1+, \dots, 9-, 9_0$ . For example, the interval 1.5 to 2.5 is divided equally into thirds, designated by 2-, 2<sub>0</sub> and 2+. The two extreme values 0<sub>0</sub> and 9<sub>0</sub> comprise only one-sixth of an intensity interval and denote respectively the most quiet and the most disturbed conditions. The daily average of the 8  $K_p$  indices is called the daily planetary index  $K_p$  and it is often taken as a daily figure for the world average geomagnetic disturbance grade. This index describes the average geomagnetic activity very well, except for the regions near the poles.

Corresponding to each 3-hourly  $K_p$  index there is the 3-hourly planetary amplitude index  $a_p$ , which can be interpreted as the mean amplitude variation corresponding to a given level of  $K_p$ . The index  $a_p$  has a linear scale (in unit of 2 nT) and can be obtained from  $K_p$  using the conversion given in Table 3. The average of the 8 values of  $a_p$  for a day is the daily planetary amplitude  $A_p$ , ranging from 0 to 400 (in nanoTeslas).

The antipodal index aa is obtained by averaging a linearisation of the K-indices from the station of Hartland (UK) and Canberra (Australia), which are roughly antipodal observatories. It has been computed retrospectively to 1868. The aa index data set extends over approximately eleven solar cycles and so potentially provides more information on correlation of geomagnetic and solar activity than  $K_p$  which is restricted to five cycles.

### 2.3 The Data Set Assembled

The data set assembled comprises monthly mean values of sunspot numbers, (recorded since January 1749) the F10.7 solar radio flux (recorded from February 1947),

the aa index (from January 1868) and the  $a_p$  index (starting January 1932).

$K_p$	$a_p$
0 <sub>0</sub>	0
0+	2
1-	3
1 <sub>0</sub>	4
1+	5
2-	6
2 <sub>0</sub>	7
2+	9
3-	12
3 <sub>0</sub>	15
3+	18
4-	22
4 <sub>0</sub>	27
4+	32
5-	39
5 <sub>0</sub>	48
5+	56
6-	67
6 <sub>0</sub>	80
6+	94
7-	111
7 <sub>0</sub>	132
7+	154
8-	179
8 <sub>0</sub>	207
8+	236
9-	300
9 <sub>0</sub>	400

Table 3. Conversion between  $K_p$  and  $a_p$

The sources of the data are the National Geosciences Data Center in Boulder, the World Data Center for Geomagnetism in Edinburgh and the International Service for Geomagnetic Indices in Paris. The data set is updated when new definitive values are obtained.

Figure 2 shows 13-month smoothed values of the sunspot number plotted from the start of sunspot cycle 1 in February 1755 to June 1988, in the current cycle, number 22. The starting times of the F10.7 flux, the aa index and the  $a_p$  index data sets are marked on the diagram to indicate the relative length of each data series. Table 4 lists the times of sunspot minima and maxima, the smoothed sunspot numbers at the cycle minimum and maximum, and the ascent and descent duration in months for each cycle beginning with cycle 1.



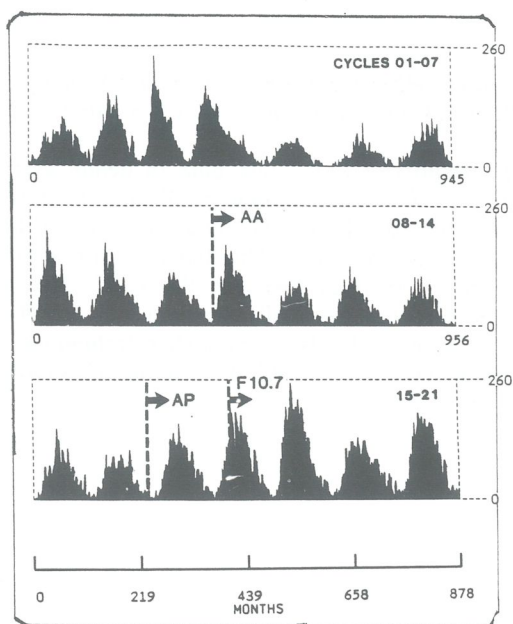


Figure 2. Monthly Sunspot Numbers from the Start of Sunspot Cycle 1

### 3. RELATIONSHIPS BETWEEN SUNSPOT NUMBER AND F10.7

The joint data set for sunspot numbers and the F10.7 index span only three complete solar cycles (17-21). A close relationship is known to exist between the two.

Smoothed F10.7 flux and sunspot numbers are plotted in Fig. 3 from February 1947 (just before the maximum of cycle 18), when F10.7 flux measurements began, to June 1988. The minima for the two data sets occur in the same month, the F10.7 flux maxima are later than the sunspot maxima in cycles 20 and 21. It is not, however, evident that the maximum value of the smoothed F10.7 flux is reached consistently later than that of the smoothed sunspot numbers. This was not the case in cycle 19, as can be seen in Figure 3.

The two data sets are clearly closely related and this is illustrated in Figure 4a, where the F10.7 flux is plotted against sunspot number. The best-fit straight line, determined by the method of least squares, is also shown.

This line is described by the equation

$$F10.7 = 59.6 + 0.90R \quad (3)$$

where F10.7 is the radio flux and R is the sunspot number.

Cycle No	Min Date	Max Date	R min	R max	Asc (m)	Des (m)
1	02 1755	06 1761	8.4	86.5	76	60
2	05 1766	09 1769	11.2	115.8	39	70
3	06 1775	05 1778	7.2	158.5	35	76
4	09 1784	02 1788	9.5	141.2	41	122
5	04 1798	02 1805	3.2	49.2	82	65
6	07 1810	05 1816	0.0	48.7	70	83
7	04 1823	11 1829	0.1	71.7	79	48
8	11 1833	03 1837	7.3	146.9	40	76
9	07 1843	02 1848	10.5	131.6	55	94
10	12 1855	02 1860	3.2	97.9	50	85
11	03 1867	08 1870	5.2	140.5	41	100
12	12 1878	12 1883	2.2	74.6	60	74
13	02 1890	01 1894	5.0	87.9	47	96
14	01 1902	02 1906	2.7	64.2	49	89
15	07 1913	08 1917	1.5	105.4	49	71
16	07 1923	04 1928	5.6	78.1	57	65
17	09 1933	04 1937	3.5	119.2	43	82
18	02 1944	05 1947	7.7	151.8	39	83
19	04 1954	03 1958	3.4	201.3	47	79
20	10 1964	11 1968	9.6	110.6	49	91
21	06 1976	12 1979	12.2	164.5	42	81
22	09 1986	-	-	-	-	-

Table 4. Maximum and Minimum of Sunspot Cycles 1 to 22

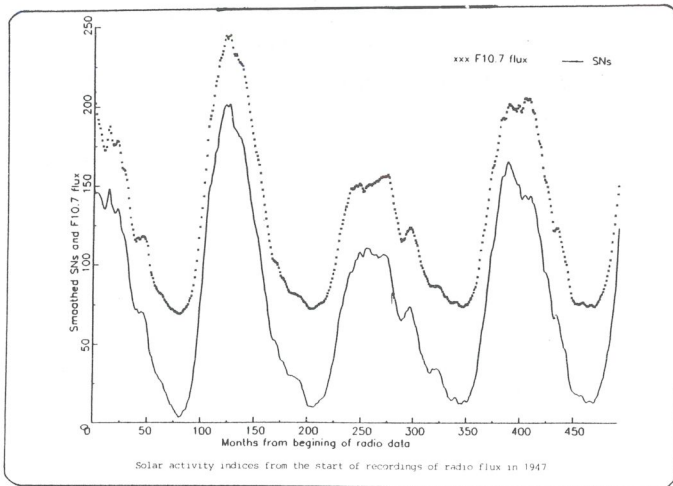


Figure 3. Solar Activity Indices from the Start of Recordings of Radio Flux in 1947.

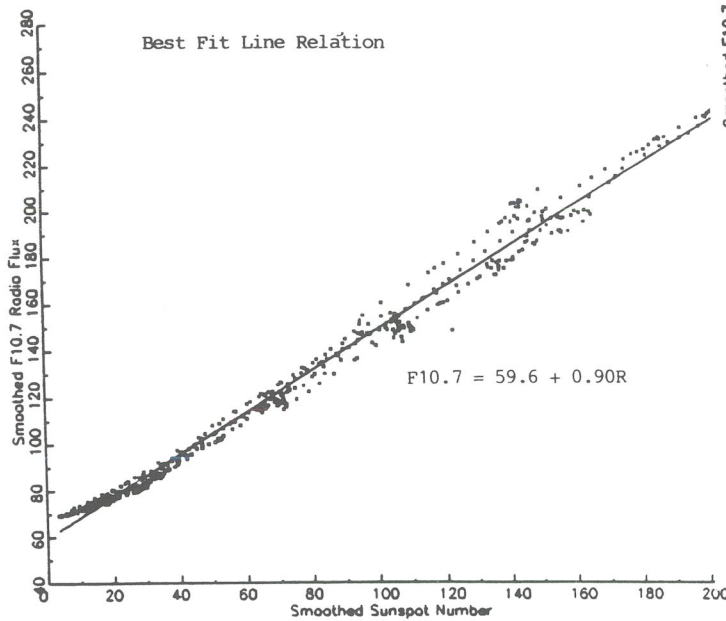


Figure 4a. Linear Relation between Sunspot Numbers and Radio Flux Data.

The best-fit quadratic is shown in Figure 4b. This has the equation

$$F10.7 = 62.2 + 0.81R + 0.00053R^2 \quad (4)$$

The overall fit of the quadratic to the data is only marginally better than the linear fit and is in fact poorer over cycles 20 and 21 than the linear fit. The rms residual of

the radio flux values from the linear fit is 5.0 units over cycles 20 and 21, for the quadratic fit it is 5.1 units.

There are insufficient F10.7 flux data to define average behaviour over a cycle, but equation (3) provides a basis for extrapolating the F10.7 flux data set backwards in time using sunspot numbers. This builds in the assumption that the relationship between the F10.7 flux and sunspot numbers was essentially the same before 1947 as it has been since. If this is so, predictive techniques can be applied directly to the F10.7 data taking advantage of recent observed data.

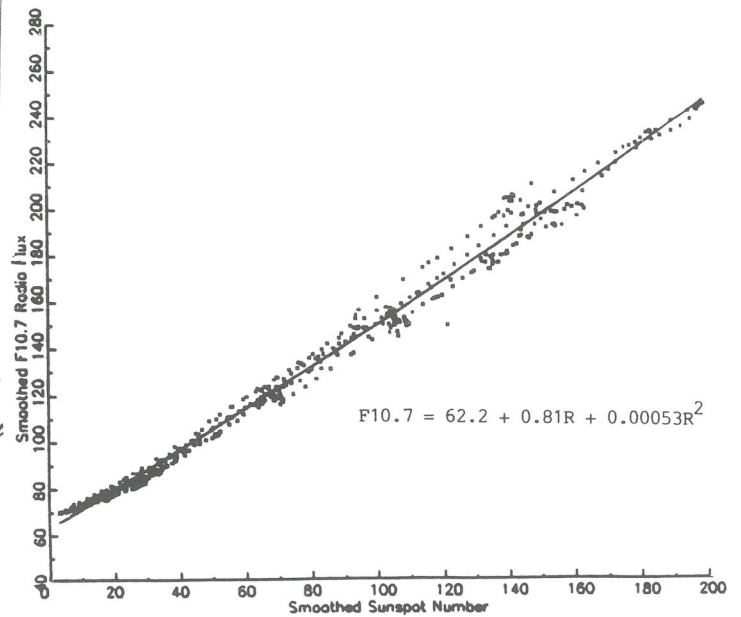


Figure 4b. Quadratic Relation between Sunspot Numbers and Radio Flux Data.

#### 4. RELATIONSHIPS BETWEEN $a_p$ AND $aa$

The joint data set for the  $aa$  and  $a_p$  geomagnetic indices span five complete solar cycles (17-21).

The ESOC requirement is for forecast values of the  $a_p$  rather than the  $aa$  index. The relation between smoothed values of  $aa$  and  $a_p$  indices for the interval 1932 to 1987 is illustrated in Figure 5. The best fit linear relation, determined by least squares, is:

$$a_p = -3.71 + 0.816aa \quad (5)$$

As with sunspot numbers and the F10.7 flux this relation provides a means for converting a prediction of the  $aa$  index into one of the  $a_p$  index.



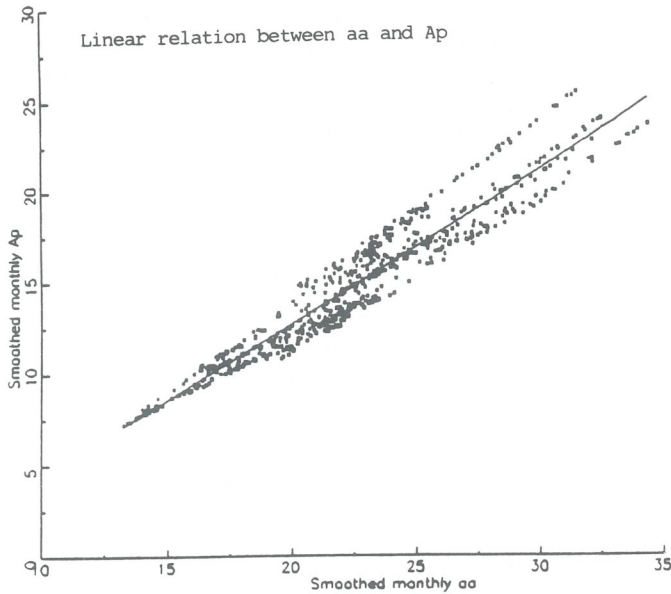


Figure 5. Linear Relation between Geomagnetic Indices.

As in the case of solar activity forecasting, the final method for prediction of the  $a_p$  index is to use as input to the prediction program the  $a_p$  data set extrapolated backwards in time to 1868 using the relationship with  $aa$  index.

## 5. FORECASTING SOLAR/GEOMAGNETIC ACTIVITY

### 5.1 Adopted Method

During the past 40 years, numerous methods have been devised to predict future levels of the solar and geomagnetic activity. The problem of prediction can be divided in two main subproblems:

- Prediction over the long-term (months to years).

Predictive mathematical techniques based on the documented long-term periodicities in sunspot numbers or 10.7 cm flux, have been developed.

- Prediction over the short-term (days).

Forecasts can be based on persistence and recurrence of activity and on direct observations of solar events and structures.

For medium- and long-term solar predictions, the techniques have been evolved along different lines. Mathematical techniques make use of linear time series and spectral models based on the historical data. The main limitation of these approaches is that the accuracy of the forecasts progressively deteriorates as the forecasts are extrapolated into the future. Other empirical techniques relate independent phenomena of the solar cycle, as for example the sunspot number or the strength of the solar polar field near the solar minimum to the future behaviour of the solar activity. These latter techniques are the

most reliable for predicting the size of the next solar cycle.

While the prediction of the maximum smoothed or monthly sunspot number varies from one method to another, for the forecasting of the time of the next solar activity maximum, the usual approach consists of using the inverse correlation between the maximum sunspot number and the solar cycle rise time. That is, the rise time is shorter when the amplitude of the solar cycle is higher.

Of the statistical techniques the longest standing is that due to McNish and Lincoln appearing firstly in 1949. As a result of the investigations conducted by the Geomagnetism Group/BGS (Edinburgh, UK) it was decided to adopt this method to satisfy the ESOC requirement of predicting the F10.7 solar flux and the  $a_p$  geomagnetic index.

The method used is a linear regression technique which has been adopted mainly for the following reasons:

- suitable for incorporation into a computer algorithm,
- based on data whose availability is assured for the future,
- well-established method, currently used by US agencies.

The data used in the forecasting software are monthly mean values of sunspot numbers, the F10.7 flux, and the  $aa$  and  $a_p$  geomagnetic activity indices. The forecasting scheme uses the data to predict smoothed monthly values of the F10.7 flux and the  $a_p$  index. The step size for the prediction is one month, thus providing a medium term forecast, and the scheme will allow monthly predictions for many years into the future so providing a long term forecast.

The problems of short-term forecasting of solar and geomagnetic activity have not yet been addressed. However, some methods which are currently applied to geomagnetic activity prediction, observations which may prove useful, and areas of research which are likely to produce results applicable to forecasting were reviewed in the study.

### 5.2 Method Implementation

The method implemented follows the approach of Holland and Vaughan (1984). The method predicts directly the (smoothed) F10.7 solar flux and the  $a_p$  index firstly extending the two data sets back to the beginning of the recordings using the relations given above.

In the implementation the following steps are taken:

1. calculate the mean period (P) of sunspot cycles 1 to 21, to the nearest month;
2. resample each cycle at P+1 points, i.e. at the same phase of each cycle, by means of an interpolation technique;
3. compute a mean cycle based on the resampled values;

4. forecast the departure from the mean cycle for month  $m$  of cycle  $c$ ,  $D_m(c)$ , using

$$D_m(c) = k_1 D_{m-1}(c) + k_2 D_{m-2}(c) + \dots \quad (6)$$

where  $D_{m-j}$  is the observed departure  $j$  months ago in the current cycle. If the series is truncated after the first term then coefficient  $k_1$ , determined by the method of least squares, is

$$k_1 = \quad (7)$$

$$\sum_{i=1}^N D_m(c-i) D_{m-1}(c-i) / \sum_{i=1}^N (D_{m-1}(c-i))^2$$

where  $N$  is the number of previous sunspot cycles included in the analysis.

The mean cycle is the starting estimate for the future cycle. Equation (6) refines the prediction under the assumption that the pattern of deviations from the mean cycle observed in previous cycles contains information relevant to the current cycle. Tests were carried out with the truncation level in the equation (6) set at values of  $i$  greater than one, but this was found to have negligible effect on forecast accuracy.

## 6. RESULTS

### 6.1 Prediction of the F10.7 Solar Radio Flux

The output of the prediction program for solar activity is a set of monthly estimates of the smoothed F10.7 solar radio flux. The performance of the adopted modified McNish and Lincoln technique was investigated.

The following testing scheme was adopted: starting with observed values up to month  $M$  a prediction was made for month  $M+6$ , the data set was then updated by one month (to month  $M+1$ ) and a prediction made for month  $M+7$ . So the testing scheme stepped through the data sets (in both the solar and geomagnetic cases) one month at a time, predicting values 6 months ahead. This scheme has been applied to prediction over cycles 20 and 21. The results are presented graphically in Figures 6 and 7 with observed values shown as a full line and predicted values shown as discrete symbols.

The overall measure of misfit is calculated from the sum of squares of the individual misfits (the quadratic or  $L_2$  norm). For  $M$  data points this is

$$\chi^2 = \sum_i [(O_i - P_i) / \sigma_i]^2 \quad (8)$$

where  $O_i$  is the  $i$ 'th observation,  $P_i$  is the predicted value. If the individual misfits could be normalised to the standard errors of each observation ( $\sigma_i$ ) the result would be the chi-squared statistic ( $\chi^2$ ), and formal statistical tests of the acceptability of a particular misfit could be adopted. Since these errors are unknown we formally set  $\sigma_i = 1$  (data unit) and determine the rms error as

$$rms = \sqrt{(\chi^2 / M)} \quad (9)$$

Figure 6 illustrates the results of applying the modified McNish and Lincoln technique, predicting 6 months ahead with a one-month step through cycles 20 and 21, to the F10.7 flux data set extrapolated back to the beginning of cycle 1. The rms error in the fit to the observed data is 6.1 flux units.

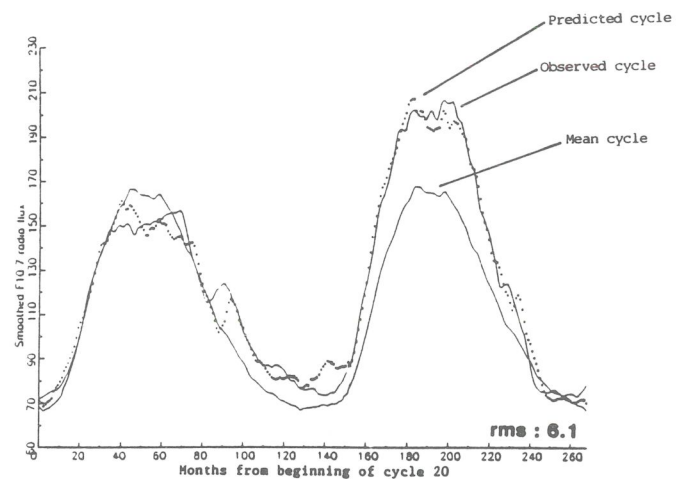


Figure 6. Predicted Radio Flux Data over Solar Cycles 20 and 21.

### 6.2 Prediction of the $a_p$ Geomagnetic Index

The output of the prediction software for  $a_p$  is a set of monthly estimates of the smoothed  $a_p$  index.

In the case of solar activity forecasting the adopted method for prediction of the F10.7 flux is to use as input to the prediction program the F10.7 flux data set extrapolated backwards in time using the relationship with sunspot numbers. The same technique has been adopted with the  $a_p$  and  $aa$  indices; the relationship expressed by equation (5) can be used to project the  $a_p$  data set to 1868. The prediction algorithm will then use the combination of observed and extrapolated  $a_p$  values rather than the  $aa$  index.

In Figure 7a the extrapolated  $a_p$  index data set is plotted and predictions, using the McNish and Lincoln algorithm, made each month for 6 months ahead, are also shown. The rms fit of the predicted values to the extrapolated data set is 2.4 units. Figure 7b shows the section of the plot for the last three cycles. The rms prediction error over the last two cycles is 2.1 units.



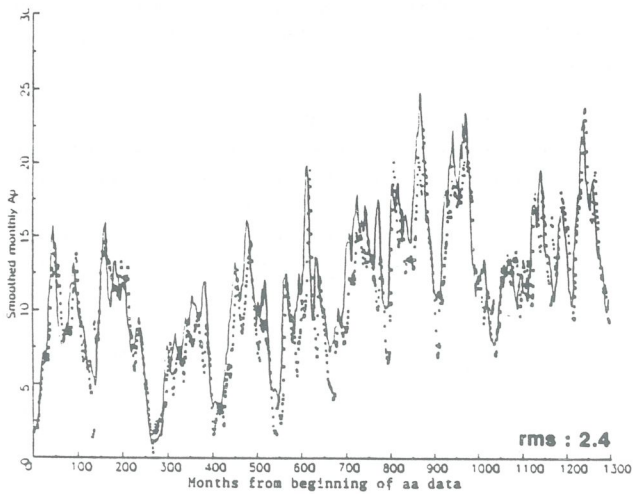


Figure 7a. Predicted  $a_p$  Index over Solar Cycles 11 to 21.

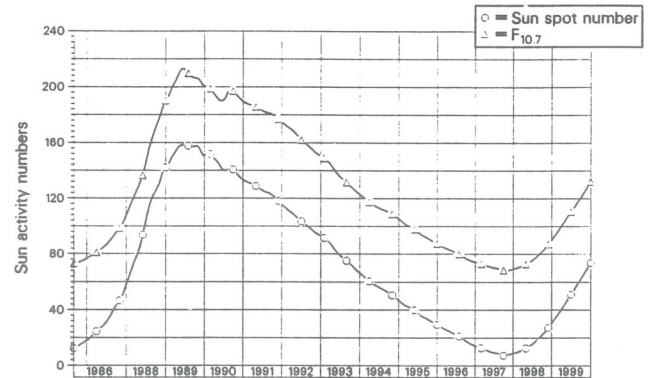


Figure 8. Predicted Solar Activity Indices over Solar Cycle 22

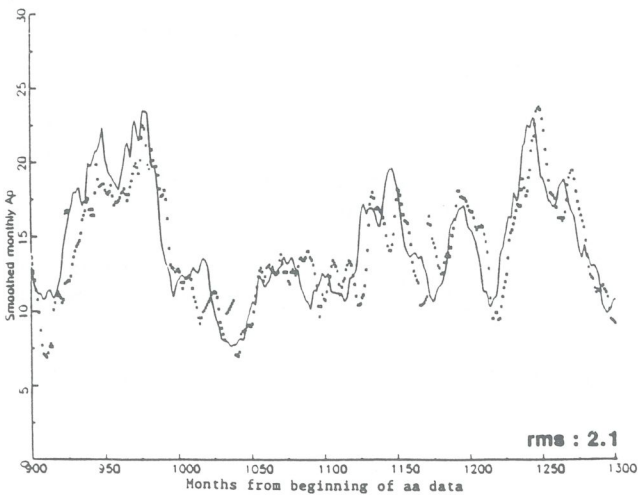


Figure 7b. Predicted  $a_p$  Index over Solar Cycles 19 to 21.

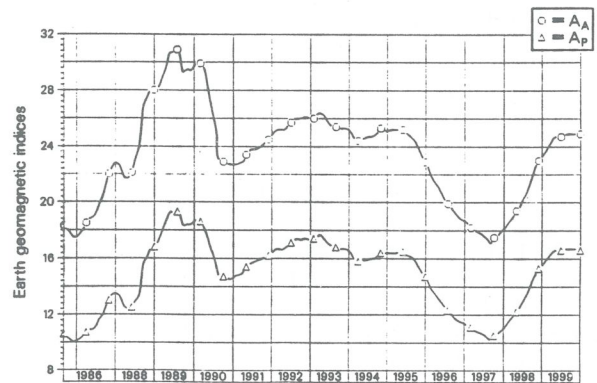


Figure 9. Predicted Geomagnetic Indices over Solar Cycle 22

### 6.3 SOLMAG

The modified McNish and Lincoln technique has been implemented in a FORTRAN program called SOLMAG which reads in monthly values of sunspot number, F10.7 flux, aa index and  $a_p$  index. The program then predicts smoothed monthly values of each series. In Figure 8 the predictions of smoothed sunspot numbers and F10.7 flux for the cycle 22 using observed monthly values up to March 1991 are shown. The minimum smoothed sunspot number will be 7.7 in October 1997 according to this forecast. Figure 9 shows the values predicted for the smoothed aa index and  $a_p$  index respectively. Geomagnetic activity is predicted to have a minimum in October 1997.

Given a prediction of future solar or geomagnetic activity in terms of the F10.7 flux or the  $a_p$  index it is important to be able to attach a confidence level to the prediction. The mean cycle and its standard deviation gives a starting point for error estimation assuming that the cycles observed so far are samples from a family of cycles forming a Gaussian distribution. However, the error is not only a function of the prediction interval, but also of the phase of the cycle at the time of the predicted value.

The rms prediction error for the F10.7 flux, calculated by applying the forecasting algorithm to cycles 1 to 21 and comparing observed and predicted values, has been computed for a range of prediction intervals. These summary statistics are used to provide the initial error estimate. This estimate is then multiplied by a factor determined from the phase in the cycle of the point of prediction. The

factor is the standard deviation at that phase of the cycle divided by the overall rms figure. Figure 10 shows the F10.7 flux prediction for cycle 22, with error bounds calculated using this scheme.

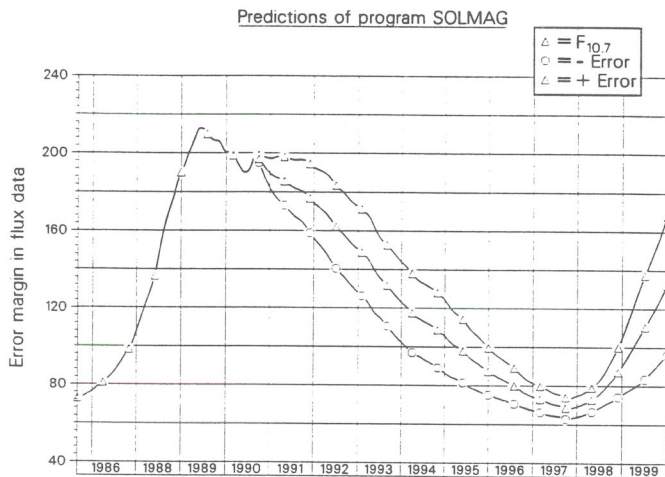


Figure 10. Predicted F10.7 over Solar Cycle 22 with Errors Bounds

## 7. SUMMARY

The SOLMAG system developed by Geomagnetism Group/BGS (Edinburgh) under ESOC contract allows long- and medium-term forecasts of the solar/geomagnetic activity as characterised by the 10.7 cm radio flux (F10.7) and  $a_p$  index. These indices are the

necessary input data for the existing air density models and their prediction can then be used for long-term planning of space missions.

The method adopted for predicting the solar/geomagnetic activity is a variant of the McNish and Lincoln technique, which is used by several U.S. agencies. The method uses monthly values of sunspot numbers, F10.7 solar flux, aa and  $a_p$  index to predict values of each series. The prediction method is a linear regression technique and makes use of all the historical data available.

The step size for the prediction is one month, thus allowing medium- and long-term forecasts. The SOLMAG system allows values from any date to be written into the output file and this enables the plotting of both observed and predicted values over any time span.

## 5. REFERENCES

1. Kerridge D., Carlaw V. and Beamish D. 1989, Development and Testing of Computer Algorithms for Solar and Geomagnetic Activity Forecasting, British Geological Survey, Technical Report WM/89/22C.
2. Mayaud P. N., 1980, Derivation, Meaning and Use of Geomagnetic Indices, Americ. Geophys. Union, Geophysical Monograph 22, Washington DC: American Geophysical Union, 154 pp.
3. McNish A. G. & Lincoln J. V., 1949, Prediction of Sunspot Numbers, Trans. Am. Geophys. Union, 30, 673-685.
4. Mugellesi R., 1987, Review of Solar/Geomagnetic Predictive Methods for Air Density Computations, ESOC OAD WP No. 349.